Available online at www.sciencedirect.com
SCIENCE DIRECT®
Biochimica et Biophysica Acta 1670 (2004) 40–48
BIOCHIMICA ET BIOPHYSICA ACTA
BBA
www.bba-direct.com

Modulation of porphyrin binding to serum albumin by pH

Pavel Kubát[a], Kamil Lang[b], Pavel Anzenbacher Jr.[c,*]

[a] J. Heyrovský Institute of Physical Chemistry, Academy of Sciences of the Czech Republic, Dolejškova 3, 182 23 Prague 8, Czech Republic
[b] Institute of Inorganic Chemistry, Academy of Sciences of the Czech Republic, 250 68 Řež, Czech Republic
[c] Department of Chemistry and Center for Photochemical Sciences, Overman Hall, Bowling Green State University, Bowling Green, OH 43403, USA

Received 8 July 2003; received in revised form 6 October 2003; accepted 10 October 2003

Abstract

In this study, we show that the difference in acidity of functional groups in porphyrin photosensitizers provides a meaningful avenue to achieve differential localization and retention of porphyrins in tissues and cells, and in the end could be a positive factor in the photodynamic treatment of cancer (PDT). We have demonstrated that *meso*-tetraphenylporphyrin derivative with four phosphonate ($-P(=O)(-OH)_2$) moieties exists in aqueous solutions mainly in four forms that differ by a degree of protonation of the porphyrin ring and ionization of the phosphonate group. It is shown that each porphyrin form has different affinities toward the model protein (bovine serum albumin, BSA). Thus pH of the medium significantly modulates the affinity of the phosphonate porphyrin toward BSA. At lower pH (pH 6.0), the phosphonate porphyrin and BSA form a complex with affinity constant of $K_b = 6.9 \times 10^5\ M^{-1}$, while at pH 7.0 the $K_b = 6.1 \times 10^5\ M^{-1}$. At pH 8.0 the association is significantly lower. Because cancerous cells have generally lower pH (pH ~ 6.9) compared to healthy cells (pH ~ 7.4), the pH of such cells could be a decisive factor for cellular retention of the porphyrin in the form of an associate with intracellular proteins. Moreover, we have also demonstrated that the protonation/deprotonation equilibria do not negatively affect the photophysical properties or ability of phosphonate porphyrin to generate singlet oxygen.

Keywords: Tetraphenylporphyrin; Protein; Association; Phosphonate; Singlet oxygen; Photodynamic therapy

1. Introduction

Photodynamic therapy (PDT) is a relatively new treatment of cancer based on administration of tumor-localizing photosensitizers such as porphyrins, phthalocyanines, chlorines, and others compounds, and their subsequent activation by red light to destroy cancer cells [1,2]. Activation of the porphyrin photosensitizer leads to the formation of porphyrin triplet states and singlet oxygen, the main cytotoxic species in PDT. In order to achieve a sufficiently high level of tumor eradication without any damage to the healthy tissue, one has to use a sensitizer that preferentially localizes in tumors. In principle, tumor localization of a sensitizer may be achieved by attaching a protein and oligopeptide or oligonucleotide fragments with sequences that are recognized by the tumor-cell receptors [3]. However, the attendant difficulties with the preparation of such bioconjugates as well as their generally low chemical and metabolic stability make this approach less viable for practical applications. Here, the approach that utilizes pre-association of a sensitizer with endogenous carriers such as serum albumin in blood followed by dissociation of the complex inside the cell during the metabolic processes seems to be particularly appealing. The differences in acidity (~ pH) between healthy and cancerous cells might be utilized to increase the stability of the carrier–porphyrin complex, thus increasing the efficacy in transport of negatively charged porphyrins which otherwise would not be transported effectively into cells. Such an increase in an in-cell transport may help in accumulation of the porphyrin drug in the cells of cancerous tissues, thus improving a chance for a successful PDT. This notion is supported by recent reports that show that while the median of pH in a healthy tissue is circa 7.4, the microenvironment in tumors is generally more acidic with median pH values of about 6.9 [4,5]. We believe that this difference in acidity provides a meaningful avenue to achieve the differential acidity-based localization in tissues, and in the end could be useful in the treatment of cancer [4].

* Corresponding author. Tel.: +1-419-372-2080; fax: +1-419-372-9809.
E-mail address: pavel@bgnet.bgsu.edu (P. Anzenbacher).

0304-4165/$ - see front matter © 2003 Elsevier B.V. All rights reserved.
doi:10.1016/j.bbagen.2003.10.011

However, the utilization of the dissociation/ionization and association with endogenous protein carriers to improve drug accumulation in tumors is predicated upon detailed understanding of ionization of various suitable porphyrins and association with proteins, which is the subject matter of this study.

Serum proteins are known to serve as endogenous carriers for various drugs [6,7], and are expected to facilitate selective delivery of the porphyrin to tumors. Specifically, the nonpolar porphyrins are bound mainly to serum lipoproteins [8], while water-soluble polar porphyrins form complexes with serum albumin [6]. Examples are deuteroporphyrin IX [9] and various derivatives of *meso*-tetraphenylporphyrin substituted by sulfonato- [10–12] and carboxy methyleneoxy groups [13], and groups that are known to associate strongly with serum albumins. Porphyrin–serum albumin complexes are presumably stabilized by electrostatic interactions between negatively charged substituents on the porphyrin periphery and positively charged ammonium residues of serum albumin. Unfortunately, the pK_a values of groups, such as $-SO_3H$, $-OH$, $-COOH$, usually used in porphyrins do not allow for successful utilization of such derivatives in the "physiological" range of pH.

For this reason, we synthesized the *meso*-tetraphenylporphyrin derivative substituted with phosphonic groups (TPPP, see Fig. 1). Dissociation constants for the $-P(OH)(OH) \rightleftharpoons -P(OH)(O^-) \rightleftharpoons -P(O^-)(O^-)$ equilibrium in arylphosphonic acids exhibit values of p$K_1 \sim 2$ and p$K_2 \sim 7$ [14] while showing modest changes depending on substitution of the aromatic ring. Therefore, we expected that in the neutral region of pH our porphyrin tetraphosphonate would display an equilibrium between the tetraanion $TPPP(OH)_4(O^-)_4$ and octaanion $TPPP(O^-)_4(O^-)_4$.

In this study, we concentrate on several key factors associated with utilization of TPPP as a photosensitizer, e.g. association of TPPP with potential endogenous carrier proteins such as serum albumin and its dependence on pH. We demonstrate that the pH of the medium significantly modulates the affinity of the phosphonate porphyrin toward proteins. Because cancerous cells have generally lower pH (pH ~ 6.9) compared to healthy cells (pH ~ 7.4), the pH of such cells could be a decisive factor for cellular retention of the porphyrin in the form of an associate with intracellular proteins. Last but not least, we examine the ability to generate cytotoxic species (singlet oxygen and triplet states of porphyrin) at different pHs and show that the changes of pH do not affect the ability of TPPP to generate singlet oxygen.

2. Materials and methods

2.1. Chemicals

5,10,15,20-Tetrakis(4-sulfonatophenyl)porphyrin tetrasodium salt (TPPS, Aldrich), bovine serum albumin, fraction V (BSA, Merck), and D_2O (98%) were used as received. NMR spectra were recorded using Varian Unity 400 MHz instrument in acetone-d_6 and referenced to the same solvent. Chemical shifts are listed in delta scale, interaction constants are in hertz.

2.2. Synthesis of 5,10,15,20-tetrakis(4-phosphonatophenyl) porphyrin, TPPP

Starting 5,10,15,20-tetrakis(4-bromophenyl)porphyrin was prepared according to the literature [15]. This porphyrin

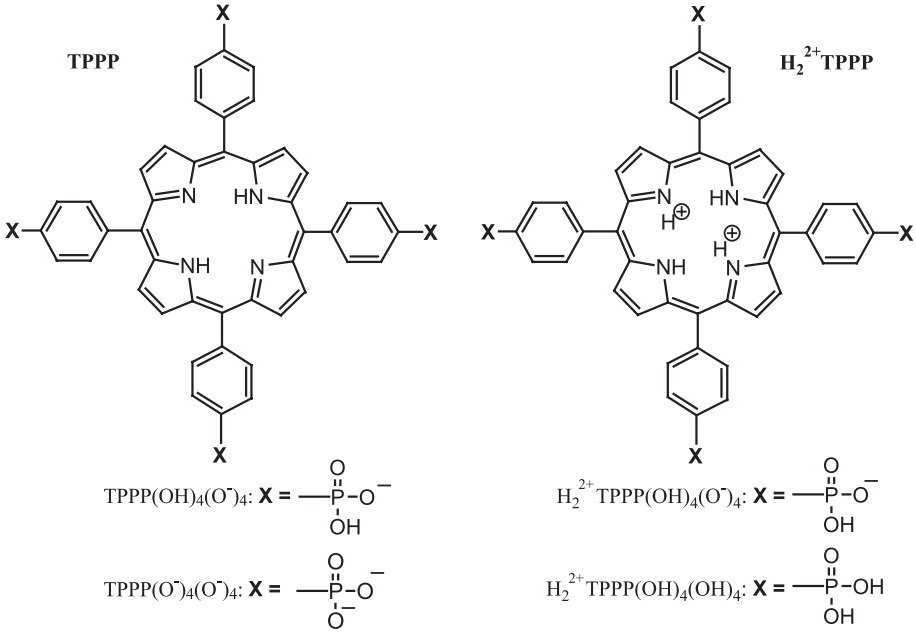

Fig. 1. Molecular structures of TPPP forms present in aqueous solutions.

was converted to the respective phosphonate octaethyl ester according to the method by Hirao et al. [16]. Tetrabromoporphyrin (0.994 g, 1.0 mmol), diethylphosphite (0.608 g, 4.40 mmol), and triethylamine (0.445 g, 4.40 mmol) were dissolved in a tetrahydrofuran-toluene mixture (1:1, 200 ml), purged with argon, and $Pd(PPh_3)_4$ was added. The reaction mixture was refluxed for 2 days. The product was purified using column chromatography (silica, 4% methanol in dichloromethane). The last violet fraction yielded the desired product (320 mg, 28%).

^{1}H-NMR: −2.78 (brs, 2H, NH), 1.47 (t, 24H, J=6.9, CH_3), 4.34 (m, 16H, OCH_2), 8.24 (m, 8H, *m*-CH), 8.42 (m, 8H, *o*-CH), 8.91 (brs, 8H, pyrrole-CH). ^{13}C-NMR: 16.82 (J=6.1, CH_3), 62.83 (J=6.1, CH_2), 120.35, 129.10, 130.98 (J=9.9, *o*-CH), 135.27 (J=15.3, *m*-CH), 146.48, 196.72. MS (ESI): 1161 (M+H).

The octaethyl ester of TPPP (40 mg, 0.344 mmol) was converted to a free acid by treatment with bromotrimethylsilane (52 mg, 3.44 mmol) in absolute acetonitrile (40 ml) for 4 days at 40 °C. A dark violet-green precipitate was filtered off, washed with acetonitrile, redissolved in deionized water, and evaporated to dryness. HPLC (C18, H_2O-AcCN gradient) showed a single peak with corresponding molecular mass (ESI) of 936 (M+H). The yield was 31 mg (96%).

2.3. Spectroscopic measurements

All UV/VIS absorption spectra were recorded using a Perkin Elmer Lambda 19 spectrophotometer. The acido-basic behavior was evaluated from changes in the Soret band at different pHs. For calculation of respective p*K*s, we assumed that at pH 3.0, pH 6.6, and pH 11.1, only species $H_2^{2+}TPPP(OH)_4(O^-)_4$, $TPPP(OH)_4(O^-)_4$, and $TPPP(O^-)_4(O^-)_4$, respectively, are present in the solution (Fig. 1). The binding data for porphyrin–BSA complexes were treated using the Scatchard equation:

$$r/c_F = K_b(N - r), \quad (1)$$

where r is the ratio of molar concentrations of bound porphyrin to BSA, c_F is the concentration of free (unbound) porphyrin, K_b is the binding constant of the porphyrin–BSA complex, and N is the number of identical binding sites for porphyrin. All analyses using the Scatchard equation (Eq. (1)) were averaged from three independent experiments. Porphyrin TPPP was completely bound to BSA at BSA/porphyrin molar ratio R=110 (pH 6.0). The fraction of the bound porphyrin to BSA (c_{bound}) was calculated using $c_{bound}=(A - A_{free})/(A_{bound} - A_{free})$, where A, A_{free}, and A_{bound} are absorbances of the sample (at selected R), of free (R=0), and of completely bound porphyrin, respectively.

Steady-state fluorescence spectra were recorded using a Perkin Elmer LS 50B luminescence spectrophotometer. All fluorescence emission spectra were corrected for the characteristics of the detection monochromator and photomultiplier. The absorbances of the samples were less than 0.04/1 cm cell at the excitation wavelength (ca. 520 nm). The fluorescence quantum yields were obtained by comparison of the integrated area under the emission spectra of the porphyrin samples with TPPS (Φ_f=0.060 ± 0.005[17]). All experiments were performed in air-saturated 20 mM phosphate buffer (pH 7.0) at room temperature.

Energy transfer from excited tryptophanyl residues of BSA to the bound TPPP can be estimated using Eq. (2) [18]:

$$R_o = 0.211[\kappa^2 n^{-4} Q_D J(\lambda)]^{1/6}, \quad (2)$$

where κ^2 is the orientation factor, n is the refractive index of the solvent, Q_D is the fluorescence quantum yield of BSA in the absence of TPPP, and $J(\lambda)$ is the overlap integral between the emission spectrum of BSA and the absorption spectrum of TPPP.

The fluorescence lifetime of porphyrins was measured by a single photon counting detection system at 640 nm (excited at 390 nm; IBNM Consultants, UK). Laser flash photolysis experiments were performed using a Lambda Physik FL 3002 dye laser (414–424 nm, output 0.05–5 mJ/pulse, pulse width ~28 ns). The transient spectra (300–600 nm) were recorded using a laser kinetic spectrometer (Applied Photophysics, UK). The time profiles of the triplet state decay were recorded at 450 and 510 nm using a 250 W Xe lamp equipped with a pulse unit, and a R928 photomultiplier (Hamamatsu). Time-resolved near-infrared luminescence of singlet oxygen O_2 ($^1\Delta_g$) at 1270 nm was monitored with a Ge diode (Judson J16-8SP, USA) in conjunction with a 1270 nm interference filter. The quantum yields of singlet oxygen Φ_Δ were estimated by the comparative method using TPPS as a standard (Φ_Δ=0.63) [19] at excitation energy of 350 μJ. In this energy region, the intensity of a luminescence signal is proportional to the incidental energy. Optically matched solutions at the excitation wavelength of 308 nm (A_{308}=0.100 ± 0.002) were prepared as aqueous solutions containing 50% D_2O to increase the singlet oxygen lifetime [20]. The samples were saturated by air or by oxygen, and where appropriate, oxygen was removed from the solution via argon purging.

3. Results and discussion

3.1. Ground state properties

The absorption spectra of aqueous TPPP solutions change with changing pH. This is attributed to protonation of the two porphyrin pyrrole nitrogens and/or ionization of phosphonic acids at the macrocycle periphery. The spectroscopic changes occurring at Soret and Q-bands observed at pH 2–12 suggest the presence of (at least) three spectroscopic species (see Fig. 2). The assignment of the Soret bands of the individual species was based on comparison with the acido-basic behavior of TPPS [21] and of arylphosphonic acids [14]. The expected acido-basic equilibria of the ground state of TPPP (Fig. 1) are shown in Scheme 1.

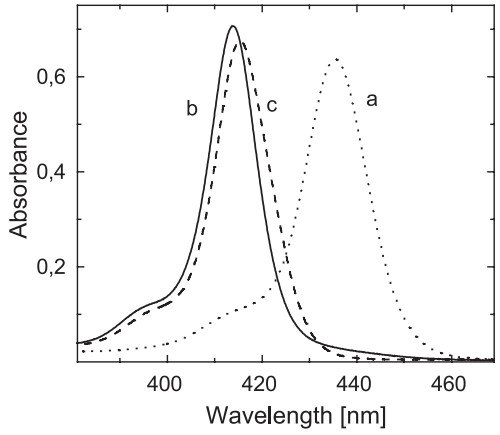

Fig. 2. Soret bands of TPPP (1.8 μM) in an aqueous solution at different pH: $H_2^{2+}TPPP(OH)_4(O^-)_4$, pH 3.0 (a), $TPPP(OH)_4(O^-)_4$, pH 6.6 (b), and $TPPP(O^-)_4(O^-)_4$, pH 11.08 (c).

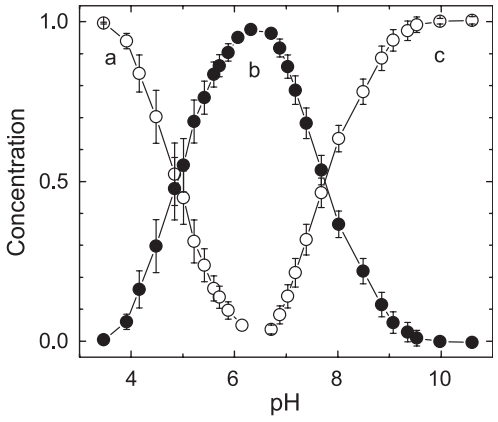

Fig. 3. Relative concentrations of respective TPPP species calculated from the spectral changes in the Soret region: $H_2^{2+}TPPP(OH)_4(O^-)_4$ (a), $TPPP(OH)_4(O^-)_4$ (b), and $TPPP(O^-)_4(O^-)_4$ (c).

We did not observe a fully protonated dication $H_2^{2+}TPPP(OH)_4(OH)_4$ because the value pK_1 is expected to be less than 2 [14]. The diprotonated porphyrin $H_2^{2+}TPPP(OH)_4(O^-)_4$ has the Soret band absorption at 435 nm and the Q-bands at 599 and 649 nm. This diprotonated species is dominating at pH 3.0 (Fig. 2a) and its spectroscopic signatures resemble the diprotonated H_2^{2+} TPPS with maxima located at 433, 592, and 644 nm. Monoprotonated $H^+TPPP(OH)_4(O^-)_4$ and diprotonated $H_2^{2+}TPPP(OH)_4(O^-)_4$ cannot be distinguished spectroscopically as individual species, presumably because both pK_2 and pK_3 are close to each other. This is supported by similar observations made using the sulfonated analogue TPPS [19,21]. The analysis of the Soret bands allows calculation of the apparent dissociation constant K_{23} of the dianion ($pK_{23} = \sqrt{pK_2 \cdot pK_3}$) (see Fig. 3a). The value of $pK_{23} = 4.8 \pm 0.2$ is comparable with that of TPPS ($pK_a = 4.9$). With increasing pH, the Soret band is shifted to 414 nm (Fig. 2b, pH 6.6) and 416 nm (Fig. 2c, pH 11.1). These changes are attributed to the formation of anions $TPPP(OH)_4(O^-)_4$ and $TPPP(O^-)_4(O^-)_4$, respectively. The formation of these species is also indicated by changes of the spectral pattern of Q-bands, specifically by the transition from a two Q-band spectrum of $H_2^{2+}TPPP(OH)_4(O^-)_4$ (D_{4h} symmetry) to a four Q-band spectrum corresponding to lower D_{2h} symmetry of the macrocycle. The dependence of the relative concentrations of both $TPPP(OH)_4(O^-)_4$ (Fig. 3b) and $TPPP(O^-)_4(O^-)_4$ (Fig. 3c) on pH allows to estimate the pK_4 value of 7.8 ± 0.1. This value is in good agreement with pK's of phosphonic groups of other arylphosphonic acids [14]. Spectral properties of all observed species $H_2^{2+}TPPP(OH)_4(O^-)_4$, $TPPP(OH)_4(O^-)_4$, and $TPPP(O^-)_4(O^-)_4$ are summarized in Table 1. The Lambert–Beer plots of respective species performed up to 20 μM were found to be linear yielding the molar absorption coefficients. These results indicate that all three species are monomeric in aqueous solutions.

3.2. Photophysical properties

The photophysical properties of TPPP species are summarized in Table 1. The lifetime of the excited singlet states of $TPPP(OH)_4(O^-)_4$ (pH 7.0) is 9.1 ± 0.1 ns, which is essentially the same as the lifetime of TPPS being 9.6 ± 0.1, recorded under the same conditions. The triplet states of $TPPP(OH)_4(O^-)_4$ and $TPPP(O^-)_4(O^-)_4$ cannot be resolved because they have the same lifetime (300, 290 μs)

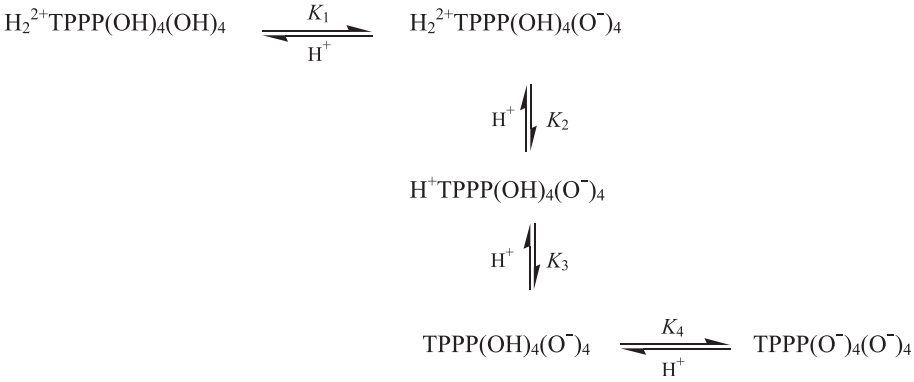

Scheme 1. Acido-basic equilibria in aqueous solution of TPPP.

Table 1
Properties of various species of TPPP

Species	pH	Ground state			Triplet states			Singlet oxygen
		λ_{max} (nm)	ε (M^{-1} cm^{-1})	pK_a	λ^T_{max} (nm)	τ_T (μs)	pK_a	Φ_Δ[a]
H_2^{2+}TPPP $(OH)_4$ $(O^-)_4$	3.0	435.0	3.1×10^5	4.8	500	180	6.0	0.54
TPPP $(OH)_4$ $(O^-)_4$	6.6	414.0	3.5×10^5	7.8	450	300	–	0.63
TPPP $(O^-)_4$ $(O^-)_4$	9.9	415.5	3.3×10^5		450	290		0.59

The maximum of the Soret band (λ_{max}) and corresponding absorption molar coefficient (ε), the maximum of triplet–triplet spectra (λ^T_{max}), the lifetime of the triplet states in the absence of oxygen (τ_T) and the quantum yield of the singlet oxygen formation (Φ_Δ).

[a] Calculated from the luminescence intensity of $^1O_2$ at 1270 nm using a standard Φ_Δ (TPPS) = 0.63 at pH 7.0 [19].

and triplet–triplet spectra (Table 1, Fig. 4a). In contrast, the diprotonated form $H_2^{2+}TPPP(OH)_4(O^-)_4$ displays a shorter triplet lifetime (180 μs) and the triplet–triplet spectrum is shifted from 450 to 500 nm (Fig. 4a and b). The triplet states of all TPPP forms are effectively quenched by molecular oxygen with the diffusion-controlled bimolecular rate constant of $1–2 \times 10^9$ M^{-1} s^{-1}. This reaction produces singlet oxygen with approximately the same efficiency for all TPPP forms characterized by the quantum yields of singlet oxygen formation Φ_Δ between 0.54 and 0.63. This result is comparable with the corresponding values of $\Phi_\Delta = 0.33–0.76$ recorded for TPPS [19,22].

The formation and decay of the triplet states of $TPPP(OH)_4(O^-)_4$ can be monitored using transient absorption at 450 nm (see Fig. 5a). When similar traces were recorded following the absorption at 510 nm (Fig. 5b), a new slow-rising part is observed, which coincides with the decrease of the $^3TPPP(OH)_4(O^-)_4$ contribution and the formation of a new species $^3H_2^{2+}TPPP(OH)_4(O^-)_4$ (Fig. 4b). This kinetic behavior was found only in the pH region between 4.0 and 6.5. Given the fact that the triplet state of porphyrin is a stronger base than the corresponding ground state [19,23] we attribute this process to the protonation of the nitrogen atoms of porphyrin in the triplet states resulting in the formation of N-protonated species. Protonation occurs with the rate constant $\sim 5 \times 10^5$ s^{-1} in 20 mM phosphate buffer at pH 6.0 and strongly competes with quenching of the $H_2^{2+}TPPP(OH)_4(O^-)_4$ and $TPPP(OH)_4(O^-)_4$ triplet states by oxygen, which has the rate constant $\sim 7 \times 10^5$ s^{-1} in an air-saturated solution. This is the reason why kinetics of protonation of the pyrrole nitrogens can be observed only in oxygen-free solutions where the rate constant of the triplet state decay is more than one order of magnitude lower ($3–5 \times 10^3$ s^{-1}). The estimated value of pK_{23} in the triplet state, calculated from kinetic traces (Fig. 5) at various pH's, is near 6. The competition between protonation/deprotonation and decay processes prevents more accurate determination of pK_{23}. The differences between ground and triplet states are most likely caused by a contraction of the porphyrin macrocycle in the triplet states originating in the rearrangement of water molecules surrounding the excited macrocycle nitrogen atoms, or by a contraction due to bonds shortening upon excitation [17].

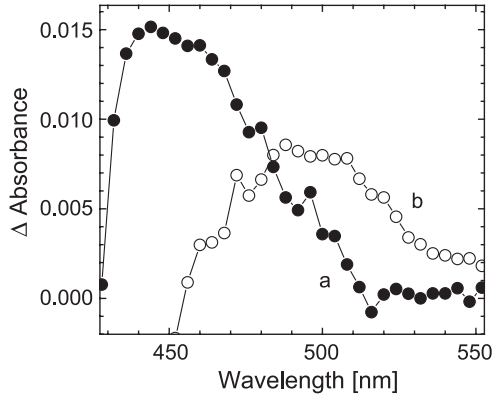

Fig. 4. Triplet–triplet difference absorption spectra of $TPPP(OH)_4(O^-)_4$, pH 7.0 (a) and $H_2^{2+}TPPP(OH)_4(O^-)_4$, pH 3.0 (b).

3.3. TPPP–BSA complex

The TPPP–BSA interaction was observed as changes in UV/VIS spectra of TPPP recorded upon addition of aliquots of BSA at pH 6.0, 7.0, and 8.0. The concentration of added BSA is expressed in molar concentration ratios BSA/porphyrin R (up to 110). In general, the addition of BSA induces a red shift in the Soret band from 414 to 420 nm (pH 6.0), and from 415 to 421 nm (pH 8.0) with some hypochromicity (see Fig. 6a and b). Likewise, the Q_x bands displayed a red shift from 582 to 592 nm, and from 636 to 646 nm, while the Q_y bands at 519 and 554 nm do not

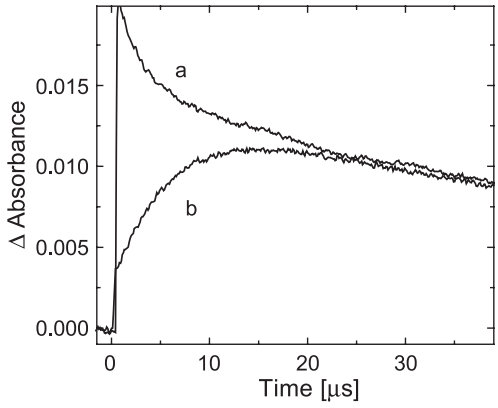

Fig. 5. Kinetic curves recorded in oxygen-free phosphate buffer, pH 6.0: decay of $^3TPPP(OH)_4(O^-)_4$ monitored at 450 nm (a), protonation of $^3TPPP(OH)_4(O^-)_4$ monitored at 510 nm (b).

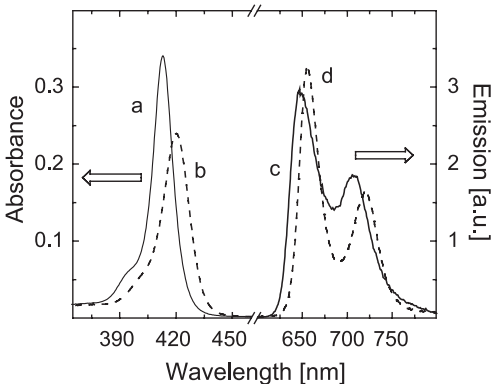

Fig. 6. Soret bands of TPPP (1.0 μM, trace a) and of the complex with BSA ($R = 110$, trace b), fluorescence spectra of TPPP (2.8 μM, trace c) and of the complex with BSA ($R = 37.1$, trace d). 20 mM phosphate buffer, pH 7.0, absorbance at the excitation wavelength $A_{518\ nm} = 0.032$/1cm cell.

appear to be significantly shifted upon the addition of BSA. Titration experiments using TPPS were carried out under identical conditions to provide a base for comparison of the binding behavior with TPPP. Since both porphyrin TPPP and TPPS are monomeric in 20 mM phosphate buffer, it is reasonable to presume that recorded spectral changes are induced only by binding of porphyrin monomers to BSA. The Soret bands show a single isosbestic point, a typical feature for the equilibrium of unbound porphyrin in a solution and bound porphyrin molecules in one type of binding site.

The changes in UV/VIS spectra are accompanied by a red shift of the fluorescence emission maxima Q(0,0) and Q(0,1) by 9 and 14 nm, respectively, as well as by the increased resolution of both peaks and decrease in the fluorescence quantum yields from 0.064 to 0.052 (Fig. 6c and d). When TPPP is completely bound to BSA the intensity of the TPPP emission spectrum obtained by excitation in the absorption band of BSA, i.e. at 280 nm ($A_{280\ nm} = 0.401$), is about two times increased compared to the experiment carried out in a BSA-free solution. In this experiment, BSA was replaced by L-tryptophan, which does not interact with TPPP, and therefore acts solely as an inner filter. Using solutions containing L-Trp or BSA of equal absorbance at 280 nm, one can directly compare the fluorescence intensities. Comparison of fluorescence intensities documents that resonance energy transfer occurs between tryptophanyl residues of BSA and TPPP within the binding sites. The Förster distance calculated using Eq. (2) is $R_o = 37.9$ or 33.8 Å, depending on the orientation factor used for the calculation: $\kappa^2 = 2/3$ (random averaging) or 0.476 (static donor–acceptor orientation during the fluorescence lifetime). Because the energy transfer efficiency is less than 10%, the presented data give the distance between the tryptophanyl residuum-bound porphyrin greater than 60–70 Å. This distance is an averaged value due to interference of two separately localized tryptophan residues (Trp^{131} and Trp^{214}). It does not allow to specify the localization of the binding site in BSA with respect to both indoles of tryptophan residues. However, it indicates that bound TPPP is in the close vicinity of at least of one tryptophan residue.

The spectral changes can be expressed in the form of the relative concentration of bound porphyrins as a function of R (see Fig. 7). The strong binding of TPPS to BSA is reflected by the sharp increase of the bound TPPS (Fig. 7d), while displaying low dependence on pH. The binding of TPPP is less effective and is considerably affected by changes in pH: the lowest TPPP–BSA affinity was recorded at pH 8.0 while the highest affinity was observed at pH 6.0 (Fig. 7a–c). Scatchard analyses performed according to Eq. (1) suggest the presence of 0.6 ± 0.3 protein binding sites with a corresponding binding constant of $(6.9 \pm 3.3) \times 10^5$ M^{-1} at pH 6.0 (see Fig. 8a) and 0.4 ± 0.1 with K_b of $(6.1 \pm 2.4) \times 10^5$ M^{-1} at pH 7.0 (Fig. 8b). Although TPPP binds to BSA in a solution of pH 8.0 (Fig. 7c), the low concentration of the bound form even at a high excess of BSA (investigated up to $R = 357$) precluded a reliable analysis of the binding data. The fact that the extent of binding decreases in solutions with high ionic strength (see Fig. 9) confirms the dominantly electrostatic origin of the binding process. As stated above, TPPS behaves quite differently. The linear Scatchard plots indicate that BSA has one binding site for TPPS ($N = 1.3 \pm 0.5$) with the binding constant of $(5.0 \pm 1.8) \times 10^6$ M^{-1}. Both parameters do not significantly depend on pH ranging from 6.0 to 8.0.

Because native BSA in solutions of pH 6.0–8.0 exists predominantly in one conformation consisting of about 55% α-helices [24], the low TPPP–BSA affinity at pH 8.0 is most likely not a result of conformational changes in the protein. This is also indirectly confirmed by TPPS binding experiments that show consistent behavior at pH 6.0–8.0. More likely, the decreased binding affinity of TPPP at pH 8.0 is related to the changes in net charge of the porphyrin as a result of protonation/deprotonation of phosphonate groups (pK_4 of TPPP is 7.8 ± 0.1). The comparison of BSA-binding properties of TPPP and TPPS yields interesting observations. The most intriguing is the fact that at pH 6.0, the dominant form $TPPP(OH)_4(O^-)_4$ (Fig. 3b), which has the same net charge and size as the tetraanionic TPPS, binds

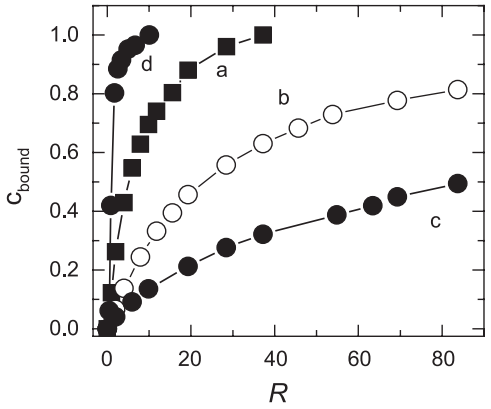

Fig. 7. Dependence of a fraction of TPPP bound to serum albumin c_{bound} on BSA/TPPP ratio R in 20 mM phosphate buffer: pH 6.0 (a), pH 7.0 (b), pH 8.0 (c) compared with that of TPPS, pH 8.0 (d). Porphyrin concentrations are 1.4 μM.

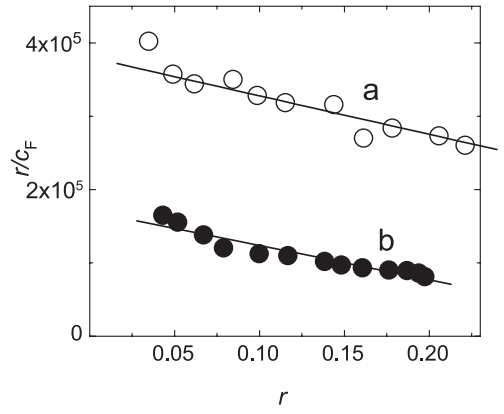

Fig. 8. Scatchard plots for binding of TPPP with BSA at pH 6.0 (a) and at pH 7.0 (b) in 20 mM phosphate buffer. Concentrations of TPPP are 1.4 μM.

to BSA with an order of the magnitude lower affinity. This suggests that other factors play an important role in TPPP–protein association. However, the only difference between sulfonate and phosphonate moieties at pH 6.0 is the presence of one extra hydrogen bond donor (P−O−H) per phosphonate moiety compared to one hydrogen bond acceptor (S=O) in sulfonate. This experimental finding may also be associated with the different ability of phosphonate and sulfonate moieties to form hydrogen bonds with protein substrates such as BSA. This view is indirectly confirmed by the observation that at pH 7.0, the $TPPP(OH)_4(O^-)_4$ still predominates (Fig. 3b), and the respective value of K_b remains unchanged. Surprisingly, the stoichiometry factor N is less than 1.0 suggesting that one porphyrin unit can interconnect with more than one BSA molecule.

A significant effect is observed at pH 8.0, close to pK_4, where the concentration of $TPPP(O^-)_4(O^-)_4$ is higher than $TPPP(OH)_4(O^-)_4$. At this pH, the ability of TPPP to associate with BSA dramatically decreases (Fig. 7c). Because the change in binding coincides with total ionization of phosphonic groups, the much weaker affinity seems to originate from the presence of dianionic phosphonate moieties.

Triplet–triplet absorption spectra of free and bound TPPP at pH 7.0 and 8.0 are very similar and do not allow to distinguish between species of a different degree of ionization. On the other hand, the time-resolved transient measurements show that the lifetimes of the triplet states of bound TPPP are much longer (>800 μs) than corresponding lifetimes of free porphyrin (300 μs). This is because TPPP is bound within an environment where the rate of solvent-enhanced triplet state deactivation to the ground state is reduced significantly compared to homogeneous aqueous solutions.

The triplet states of TPPP in an air-saturated solution at pH 7.0 displays a typical lifetime of 2.4 μs. In the presence of BSA, the oxygen-mediated quenching of the triplet states also depends on the concentration of BSA, and is best fitted by a combination of two exponential terms corresponding to two lifetimes of 2.4 and 13.8 μs. These data provide an additional evidence of a dynamic equilibrium between free (lifetime of 2.4 μs) and bound (13.8 μs) porphyrin. Generally, there is at least one porphyrin fraction considerably shielded from oxygen that displays the rate constants of the oxygen-mediated triplet quenching of about one order of the magnitude lower ($k_q \sim 10^8\ M^{-1}\ s^{-1}$) compared to that of free TPPP in a solution ($k_q \sim 10^9\ M^{-1}\ s^{-1}$). The decrease in k_q is a result of less effective collision quenching of the triplet states by oxygen. The lifetime of the bound TPPP is not dependent on pH in the range of 6.0–8.0. These results indicate that TPPP is located in the binding sites with comparable oxygen accessibility. The fluorescence decay of TPPP bound to BSA corresponds to a single long-lived fluorescence component similar to reported data for TPPS [25]. Thus, the lifetime of TPPP is extended from 9.1 ± 0.1 to 12.1 ± 0.1 ns for TPPP bound to BSA (R = 110, pH 7.0).

The presence of the protein matrix also affects the protonation of the porphyrin nitrogens in the ground and triplet states. At pH 6.0, the UV/VIS spectrum of TPPP shows a small contribution of $H_2^{2+}TPPP(OH)_4(O^-)_4$ (Fig. 3a) as a 435 nm shoulder at the Soret band of $TPPP(OH)_4(O^-)_4$. Upon binding to BSA, the N-protonated species is fully transformed to the $TPPP(OH)_4(O^-)_4$ tetraanion. The electrostatic forces seem to prevent binding of the porphyrin macrocycle in the form of a zwitterion with positively charged pyrrole nitrogens. A similar effect was observed for TPPP in the triplet states. At pH 6.0, the protonation of $^3TPPP(OH)_4(O^-)_4$ to form $^3H_2^{2+}TPPP(OH)_4(O^-)_4$ (Fig. 4b) is a dominant process. However, in the presence of BSA, protonation is not observed, and the decay traces monitored at 440–515 nm follow the same kinetics typical for bound TPPP. This is explained by the less effective diffusion of H^+ from the medium and/or from protonated amino acids in the porphyrin proximity. Inhibition of TPPP protonation in the ground and triplet states after the binding suggests that porphyrin is situated in an environment with low activity of water molecules.

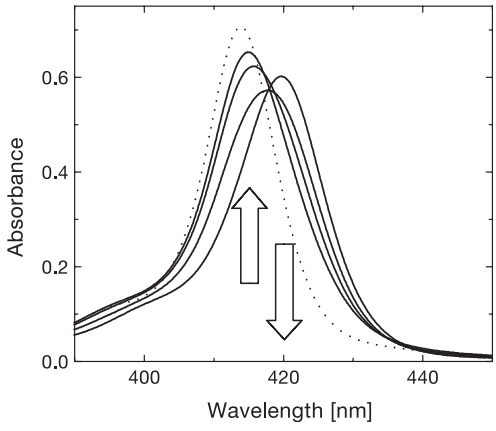

Fig. 9. Influence of ionic strength on binding of TPPP to BSA. 1.6 μM TPPP, R = 6.1, 20 mM phosphate buffer, pH 6.0, NaCl concentration: 0, 75, 270, and 480 mM, respectively. TPPP in the absence of BSA is shown for comparison (dotted line). Arrows designate absorption changes due to an increasing concentration of NaCl.

When the pH of the medium approaches pK_4 value, the changes in phosphonate group ionization and the corresponding change in the porphyrin total charge significantly affect the ability of TPPP to form complexes with BSA. The value of pK_4 for TPPP is slightly higher that the median pH values in cancer and normal tissue [4,5]. However, the acido-basic behavior of phosphonic groups can be simply modulated by adding different substituents, the method applied for a study of nucleotide binding to enzyme proteins [26,27]. The longer aliphatic chain $-(CH_2)_n-$ attached to $-PO_3H_2$ causes successive increase in pK_4 from CH_3-PO_3H_2 (pK_4 = 7.8) to $CH_3(CH_2)_3$-PO_3H_2 (pK_4 = 8.9) [14]. Similarly, significant decrease of pK_4 can be achieved by implementation of halogen atoms to the vicinity of the phosphonate moiety. For example, trihalomethane phosphonates display a gradual change in pK_4 in the following order: CI_3-PO_3H_2 (pK_4 = 6.7), CBr_3-PO_3H_2 (pK_4 = 6.5), CCl_3-PO_3H_2 (pK_4 = 4.8), and CF_3-PO_3H_2 (pK_4 = 3.9) [14].

4. Conclusions

This study demonstrates the implementation of a phosphonate moiety in the design of porphyrin photosensitizers that utilize the difference in acidity of blood plasma, healthy cells, and tumors to modulate the delivery of photosensitizers to tumors and improve drug retention in the tumors. The phosphonate moieties differ in their ionization properties from the standard sulfonate, carboxylate or phenolate groups, and as a result the phosphonate porphyrin shows different association properties with BSA. Studies of the association behavior of TPPP and BSA model confirm that perturbation of pH in the physiological range may be used to trigger or impede the association of TPPP with proteins. At lower pH (pH 6.0), the phosphonate porphyrin and BSA form a complex with affinity constant of $K_b = 6.9 \times 10^5\ M^{-1}$, while at pH 7.0 the $K_b = 6.1 \times 10^5\ M^{-1}$. At pH 8.0, the association is significantly lower. Because cancerous cells have generally lower pH (pH ~ 6.9) compared to healthy cells (pH ~ 7.4), the pH of such cells could be a decisive factor for cellular retention of the porphyrin in the form of an associate with intracellular proteins. Additionally, the modification of porphyrin with phosphonate groups does not impair the properties of the porphyrin as a photosensitizer. Experiments aimed at improving the dissociation of the porphyrin–protein complex at pH corresponding to tumors are the focus of ongoing studies.

Acknowledgements

This research was supported by the Grant Agency of the Czech Republic (grant No. 203/01/0634 to P.K. and K.L.) and NSF (DMR-0306117 to P.A.).

References

[1] T.J. Dougherty, C.J. Gomer, B.W. Henderson, G. Jori, D. Kessel, M. Korbelik, J. Moan, Q. Peng, Photodynamic therapy: review, J. Natl. Cancer Inst. 90 (1998) 889–902.
[2] I.J. Macdonald, T.J. Dougherty, Basic principles of photodynamic therapy, J. Porphyr. Phthalocyanines 5 (2001) 105–129.
[3] G. Zheng, A. Graham, M. Shibata, J.R. Missert, A.R. Oseroff, T.J. Dougherty, R.K. Pandey, Synthesis of β-galactose-conjugated chlorins derived by enyne metathesis as galectin-specific photosensitizers for photodynamic therapy, J. Org. Chem. 66 (2001) 8709–8716.
[4] I.F. Tannock, D. Rotin, Acid pH in tumors and its potential for therapeutic exploitation, Cancer Res. 49 (1986) 4373–4384.
[5] L.E. Gerweck, K. Seetharaman, Cellular pH gradient in tumor vs. normal tissue potential exploitation for the treatment of cancer, Cancer Res. 56 (1996) 1194–1198.
[6] N.A. Kratochwil, W. Huber, F. Muller, M. Kansy, P.R. Gerber, Predicting plasma protein binding of drugs: a new approach, Biochem. Pharmacol. 64 (2002) 1355–1374.
[7] F. Kratz, U. Beyer, Serum proteins as drug carriers of anticancer agents, a review, Drug Deliv. 5 (1998) 1–19.
[8] R.K. Chowdhary, I. Shariff, D. Dolphin, Drug release characteristics of lipid based benzoporphyrin derivative, J. Pharm. Pharm. Sci. 6 (2003) 13–19.
[9] M. Rotenberg, R. Margalit, Deuteroporphyrin-albumin binding equilibrium. The effects of porphyrin self-aggregation studied for the human and the bovine proteins, Biochem. J. 229 (1985) 197–203.
[10] S.M. Anrade, S.M.B. Costa, Spectroscopic studies on the interaction of a water soluble porphyrin and two drug carrier proteins, Biophys. J. 82 (2002) 1607–1619.
[11] I.E. Borissevitch, T.T. Tominaga, C.C. Schmitt, Photophysical studies on the interaction of two water-soluble porphyrins with bovine serum albumin. Effects upon the porphyrin triplet state characteristics, J. Photochem. Phototobiol., A 114 (1998) 201–207.
[12] I.E. Borissevitch, T.T. Tominaga, H. Imasato, M. Tabak, Resonance light scattering study of aggregation of two water soluble porphyrins due to their interaction with bovine serum albumin, Anal. Chim. Acta 343 (1997) 281–286.
[13] S. Chatterjee, T.S. Srivastava, Spectral investigations of the interaction of some porphyrins with bovine serum albumin, J. Porphyr. Phthalocyanines 4 (2000) 147–157.
[14] L.D. Freedman, G.O. Doak, The preparation and properties of phosphonic acids, Chem. Rev. 57 (1957) 479–523.
[15] M.M. Pereira, G. Muller, J.I. Ordinas, M.E. Azenha, L.G. Arnaut, Synthesis of vinylated 5,10,15,20-tetraphenylporphyrins via Heck-type coupling reaction and their photophysical properties, J. Chem. Soc., Perkin Trans. 2 (2002) 1583–1588.
[16] T. Hirao, T. Masunaga, Y. Ohshiro, T. Agawa, A novel synthesis of dialkyl arenephosphonates, Synthesis (Stuttg.) (1981) 56–57.
[17] T. Gensch, S.E. Braslavsky, Volume changes related to triplet formation of water-soluble porphyrins, a laser-induced optoacoustic spectroscopy (LIOAS) study, J. Phys. Chem., B 101 (1997) 101–108.
[18] J.R. Lakowicz, Principles of Fluorescence Spectroscopy, 2nd ed., Kluwer Academic Publishing/Plenum, New York, 1999, pp. 367–394.
[19] T. Gensch, T.C. Viappiani, S.E. Braslavsky, Structural volume changes upon photoexcitation of porphyrins: role of the nitrogen–water interactions, J. Am. Chem. Soc. 121 (1999) 10573–10582.
[20] P. Kubát, K. Lang, P. Anzenbacher Jr., Cationic meso-tetratolylporphyrins substituted by phosphonium groups: self-stacking and complexation to DNA, J. Phys. Chem., B 106 (2002) 6784–6792.
[21] K. Kalyasundaram, Photochemistry of Polypyridine and Porphyrin Complexes, Academic Press, London, 1992.
[22] F. Wilkinson, W.P. Helman, A.B. Ross, Quantum yields for the photosensitized formation of the lowest electronically excited singlet state of molecular oxygen in solution, J. Phys. Chem. Ref. Data 22 (1993) 113–262.

[23] P. Kubát, K. Lang, J. Mosinger, D.M. Wagnerová, Reactions photosensitized by Tetrakis(4-sulfonatophenyl) porphyrin: protonation of the triplet states and effect of amino acids, Zeit. Phys. Chem. 210 (1999) 243–256.
[24] J.F. Foster, in: V.M. Rosenoer, M. Oratz, M.A. Rothschild (Eds.), Albumin Structure, Function and Uses, Pergamon, Oxford, 1977, pp. 53–84.
[25] H. Schneckenburger, M.H. Gschwend, R. Sailer, A. Ruck, W.S.L. Strauss, Time resolved pH-dependent of hydrophylic porphyrin in solution and in cultivated cells, J. Photochem. Phototobiol., B 27 (1995) 251–255.
[26] X. Liu, Ch. Brenner, A. Churanovski, E. Starzynska, G.M. Blackburn, New tripodal, supercharged analogues of adenosine nucleotides: inhibitors for the Fhit Ap3 A hydrolyse, Angew. Chem., Int. Ed. 38 (1999) 344–347.
[27] A. Dikiy, E.G. Funhoff, B.A. Averill, S. Ciurli, New insights into the mechanism of purple acid phosphatase through ^{1}H NMR spectroscopy of the recombinant human enzyme, J. Am. Chem. Soc. 124 (2002) 13974–13975.